DECADE QUAD MONOLITHIC POS MODELING*

John Thompson, Philip Coleman, Don Parks, and Eduardo Waisman
Alameda Applied Sciences Corporation, San Diego, CA

W. Rix+
SPAWAR, San Diego, CA

Mark Babineau, Van Kenyon, and G. Lavell Whitehead
Sverdrup Technology, Tullahoma, TN

Patrick Corcoran, Randy Crumley, Michael Danforth, John Douglas, Philip Spence, Paul Steen, and Terry Tucker
Titan Pulsed Sciences Division, San Diego & San Leandro, CA

Peter Kurucz and Ken Ware
Defense Threat Reduction Agency, Alexandria, VA

Abstract

The Decade Quad (DQ) was initially fielded as a large area bremsstrahlung (LAB) source. This utilized the four Decade modules (DM) triggered simultaneously but each driving a separate hard x-ray bremsstrahlung radiation source (BRS). Recently, water convolute hardware was installed that combines the power from the four Decade modules to drive a soft x-ray plasma radiation source (PRS). The water convolute configuration also enables the use of a monolithic plasma opening switch (MPOS) for driving a common BRS or PRS load.

The work reported here was performed in support of the use of an ACE 4 type POS on DQ. The modeling included equivalent circuit and DELTA-CREMIT magneto-hydrodynamic (MHD) simulations. The circuit analysis extracted equivalent circuit parameters from ACE 4 data and applied them to the planned DQ MPOS-BRS configuration. The MHD analyses evaluated strategies to optimize the DQ MPOS.

I. DQ MPOS APPROACH

POS scaling on large pulsed power drivers has always been problematic, as scaling implies an understanding of the dominant physics of the POS. A modeler must identify the dominant physics - erosion or Hall MHD or MHD – and each of these may apply in a different part of the POS. A full understanding of POS physics, especially at the higher power levels of DM and DQ drivers, has yet to be achieved. Fully integrated modeling of even the known physics is not yet practical.

The applicability of the ACE 4 POS for the DQ MPOS is based on the observed performance of ACE 4 with both BRS and PRS loads[1,2]. Simulations and experimental results suggest that one important parameter characterizing an ACE 4 type POS is the I_C*T_C product where I_C is the peak conducted current and T_C is the conduction time. This corresponds to MHD dominance during the conduction phase. The ACE 4 POS experience includes the 2.4 MA-μs I_C*T_C product of the DQ MPOS (8 MA in 300 ns). Calculations and interferometry imply that many of the critical plasma conditions at the onset of POS opening are closely preserved if the I_C*T_C product is held constant. In addition, the circuit analysis of Section II suggests that the performance of the ACE 4 POS is not far from that required of the DQ MPOS.

Modeling of the ACE 4 POS has nearly quantitatively reproduced the observed plasma conditions at the onset of opening. They also have shown that these plasma conditions are strongly dependent on initial conditions and geometry. This offers an opportunity to investigate DQ MPOS optimization computationally in advance of experiments, as will be presented in Section III.

II. MPOS CIRCUIT MODELING

Figure 1 shows the POS-BRS geometry being implemented on DQ. On ACE 4, diagnostics implied that this configuration exhibits a two-switch, primary/secondary, composite nature as reflected in the equivalent circuit of Figure 2. There are insufficient experimental data to uniquely determine the characteristic circuit parameters t_{Open}, $Zflow_{Peak}$, and $t_{Closing}$; the opening time, peak Zflow, and closing time for both switch regions and L_{DS}, the inductance remaining downstream of the secondary switch opening region.

* Work supported by the Defense Threat Reduction Agency
+ Formerly with Maxwell Physics International

0-7803-7120-8/02/$17.00 © 2002 IEEE

Report Documentation Page

Form Approved
OMB No. 0704-0188

1. REPORT DATE	2. REPORT TYPE	3. DATES COVERED
JUN 2001	**N/A**	**-**

4. TITLE AND SUBTITLE	5a. CONTRACT NUMBER
Decade Quad Monolithic Pos Modeling	5b. GRANT NUMBER
	5c. PROGRAM ELEMENT NUMBER
6. AUTHOR(S)	5d. PROJECT NUMBER
	5e. TASK NUMBER
	5f. WORK UNIT NUMBER
7. PERFORMING ORGANIZATION NAME(S) AND ADDRESS(ES) **Alameda Applied Sciences Corporation, San Diego, CA**	8. PERFORMING ORGANIZATION REPORT NUMBER
9. SPONSORING/MONITORING AGENCY NAME(S) AND ADDRESS(ES)	10. SPONSOR/MONITOR'S ACRONYM(S)
	11. SPONSOR/MONITOR'S REPORT NUMBER(S)

12. DISTRIBUTION/AVAILABILITY STATEMENT
Approved for public release, distribution unlimited

13. SUPPLEMENTARY NOTES
See also ADM002371. 2013 IEEE Pulsed Power Conference, Digest of Technical Papers 1976-2013, and Abstracts of the 2013 IEEE International Conference on Plasma Science. IEEE International Pulsed Power Conference (19th). Held in San Francisco, CA on 16-21 June 2013. U.S. Government or Federal Purpose Rights License., The original document contains color images.

14. ABSTRACT
The Decade Quad (DQ) was initially fielded as a large area bremsstrahlung (LAB) source. This utilized the four Decade modules (DM) triggered simultaneously but each driving a separate hard x-ray bremsstrahlung radiation source (BRS). Recently, water convolute hardware was installed that combines the power from the four Decade modules to drive a soft x-ray plasma radiation source (PRS). The water convolute configuration also enables the use of a monolithic plasma opening switch (MPOS) for driving a common BRS or PRS load. The work reported here was performed in support of the use of an ACE 4 type POS on DQ. The modeling included equivalent circuit and DELTA-CREMIT magneto-hydrodynamic (MHD) simulations. The circuit analysis extracted equivalent circuit parameters from ACE 4 data and applied them to the planned DQ MPOSBRS configuration. The MHD analyses evaluated strategies to optimize the DQ MPOS.

15. SUBJECT TERMS

16. SECURITY CLASSIFICATION OF:			17. LIMITATION OF ABSTRACT	18. NUMBER OF PAGES	19a. NAME OF RESPONSIBLE PERSON
a. REPORT	b. ABSTRACT	c. THIS PAGE			
unclassified	**unclassified**	**unclassified**	**SAR**	**4**	

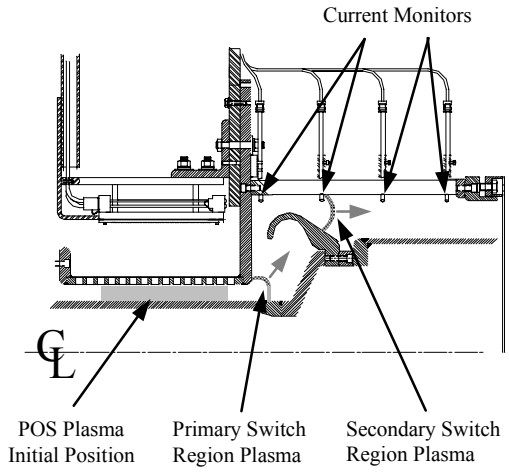

Figure 1. ACE 4 "Catcher's Mitt" POS geometry.

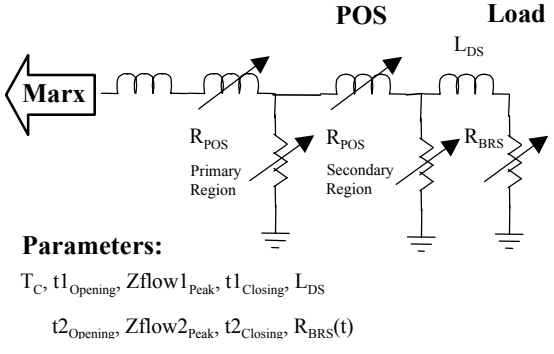

Figure 2. Equivalent circuit explicitly displaying the two region opening nature of the ACE 4 type POS.

Since we expect that the net open impedance of the POS is set by the secondary switch, we adopt for the purposes of the following analysis, the simpler equivalent circuit of Figure 3. This circuit takes into account the inductance between the primary and secondary switch regions by lumping it in with the inductance upstream of the switch.

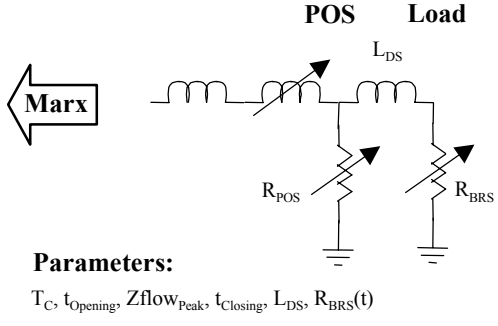

Figure 3. Simplified equivalent circuit utilizing a single "equivalent lumped circuit" POS.

A comparison of the results from such a simplified equivalent circuit and the experimental data show reasonable agreement during the opening time of the secondary switch as shown in Figure 4. The differences prior to secondary switch opening are primarily due to our accounting of the inter-switch inductance and does not affect the determination of the POS opening parameters. We used the commercial circuit simulation code, MicroCap, for our calculations. Non-standard circuit elements, the POS and e-beam diode in particular, were modeled incorporating the relevant parameters.

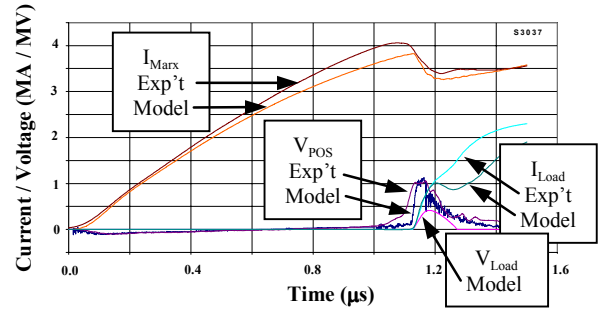

Figure 4. Typically good agreement between model and experimental data is seen during POS opening.

Table 1 gives POS parameters derived from a number of shots with both shorted and active loads. Table 1 also reflects an observed conditioning effect seen in the first few shots taken with a newly machined cathode. The circuit analysis results imply that the POS opening parameters are relatively independent of both the I_C*T_C product and the load impedance, but are affected by initial conditioning.

Table 1. Derived POS parameters for unconditioned (UC) and conditioned (C) POS cathodes.

Load	UC /C	Shot #	I_C*T_C (MA-μs)	t_{Open} (ns)	Z_{Peak} (Ω)
Shorted Diode	UC	2840	2.3	30	0.22
	UC	3018	4.7	25	0.20
	C	2848	5.0	15	0.26
e-Beam Diode	C	3037	4.5	15	0.26
	C	3048	5.0	15	0.25

Figure 5 shows an example of the application of the simplified equivalent circuit to the DQ MPOS. The objective was to deliver 290 kJ to the e-beam load. This required that the $Zflow_{Peak}$ be increased by a factor of two above the ACE 4 result to 0.5 Ω. Also, the POS-to-BRS inductance needed to be reduced by a factor of two. The first requirement implies that the switch behavior needs to be improved; see Section III. The second requirement can likely be met more easily; the ACE 4 results implied that the unoptimized inductance between the secondary switch region and the e-beam load could be reduced significantly.

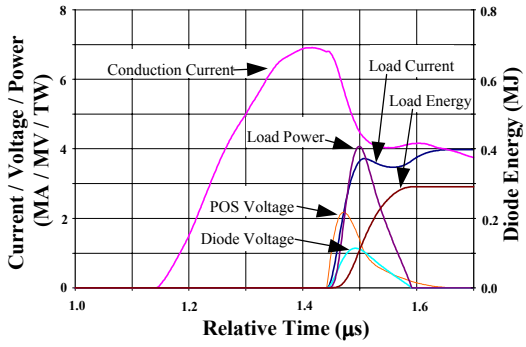

Figure 5. DQ circuit simulation that delivers 290 kJ to the BRS load.

III. MPOS OPTIMIZATION

As noted above, successful use of the ACE 4 POS on DQ will require a factor of two increase in the open impedance of the POS. We review here MHD models of ACE 4 experiments that suggest very practical methods to achieve that goal.

Figure 6 shows the ACE 4 POS-to-BRS configuration (rotated 90 degrees counterclockwise relative to Figure 1) with an overlay of the measured 2D chordal, line-integrated electron density observed during opening. The density data show the presence of a low density plasma that bridges a gap between the forward propagating, snowplowed POS plasma and the anode. The apparent secondary opening region as inferred by current probe measurements is cartooned. We conjecture that the secondary switch plasma originates from the plasma bridge. We also expect that the open impedances of both switch regions are controlled by the magnitudes of their plasma densities.

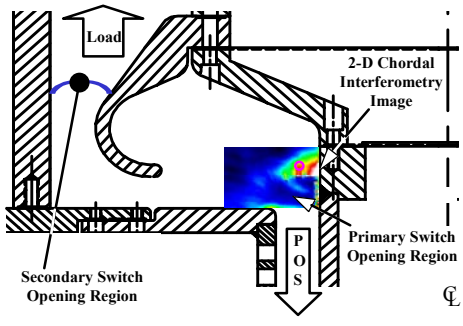

Figure 6. ACE 4 characterized POS-BRS configuration showing the observed density profile of primary switch region plasma. (The secondary switch opening region is inferred).

Using the coupled MHD and radiation/ionization modeling of the DELTA and CREMIT codes, Thompson[1,2] has shown that many of the features of the density data of Figure 6 can be reproduced in the models, in particular the low density plasma bridge. If we can reduce the density of that bridge, then we have a strategy for increasing the open impedance of the POS.

Using the MHD code, a number of variations in the POS geometry were studied to see how the plasma bridge density varied. The calculations were performed in the ACE 4 parameter space to retain a close connection to the existing experimental data. Under I_C*T_C = constant scaling, the trends if not the quantitative changes, should transfer to the DQ MPOS.

Figure 7 shows two promising geometries investigated for BRS and PRS loads. The figure also depicts alternative 2D POS anode models used in an attempt to bracket the behavior of the real 3D POS mesh anode structure. It turned out that to first order, the results were independent of the choice in modeled anode geometry.

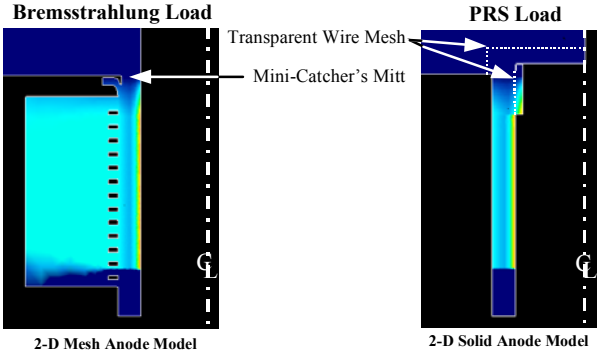

Figure 7. Geometries evaluated for MPOS optimization for BRS (left) and PRS (right) loads.

For the BRS load configuration, a "mini-catcher's mitt" –like, plasma trap was implemented on the anode. This reduced the contribution to the bridge plasma due to plasma snowplowed into and sliding along the anode surface during the conduction phase. A DELTA-CREMIT simulation is shown in Figure 8 indicating the location of the mass density lineouts. During the expected opening time, both the peak and line-integrated bridge plasma mass density profiles are reduced by a factor of 3-4 compared to the geometry of Figure 6. A reduction of this magnitude should significantly improve the opening in both the primary and secondary switch regions.

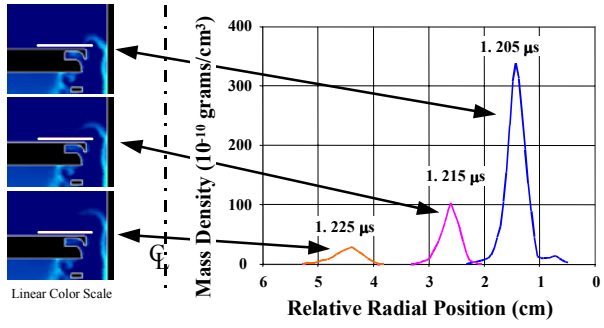

Figure 8. Typical plasma bridge density profiles near anode for an optimizing BRS load geometry.

The prospect that POS-BRS coupling can be optimized with the appropriate POS geometry leads us to expect that coupling to a soft x-ray PRS load may also be improved. But for POS-to-PRS optimization, the strategy is somewhat different. Figure 9 shows a POS driven PRS configuration that was tested on ACE 4; the figure includes an overlay of the forward propagating, snowplowed plasma as measured in the POS-BRS configuration. Here opening at the anode is problematic in that the lower density bridge plasma (where primary opening is believed to occur) interacts with the return current anode structure. Additionally, the downstream current path to the PRS load is typically shorted out by the forward propagating, snowplowed plasma along the cathode before the PRS implosion is complete. Optimization for a PRS load would therefore require the opening near the cathode rather than the anode.

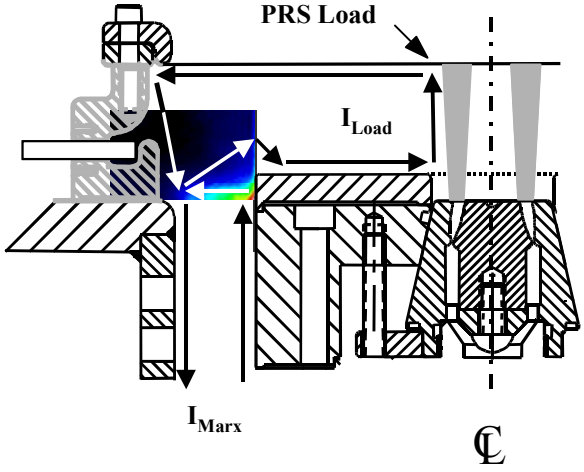

Figure 9. ACE 4 characterized POS-PRS configuration (chordal density profile from BRS shots)

For PRS load optimization using the MHD codes, the downstream cathode geometry was modified with a transparent boundary condition at the cathode surface as shown in Figure 7. Experimentally, this would be implemented by a highly transparent axially oriented wire array. Here, a "mini-catcher's mitt" -like plasma trap geometry is in the cathode. This configuration reduces the downstream plasma density near the cathode encountered by the snowplowed POS plasma. The surface pile-up normally associated with the cathode surface is then interior to the effective cathode surface. This change allows the snowplow front near the cathode to advance more rapidly, becoming nearly perpendicular to the cathode as it runs off the electrode end, reducing the inward radial component of the snowplowed plasma. This should enable opening near the cathode in the same way that modeling suggests of the formation of the low density bridge at the anode in the bremsstrahlung case.

Figure 10 shows the results of a MHD simulation for the PRS case. This configuration flips the low density bridge from the anode to the cathode. This offers the possibility of both better opening and elimination of early time switch shorting.

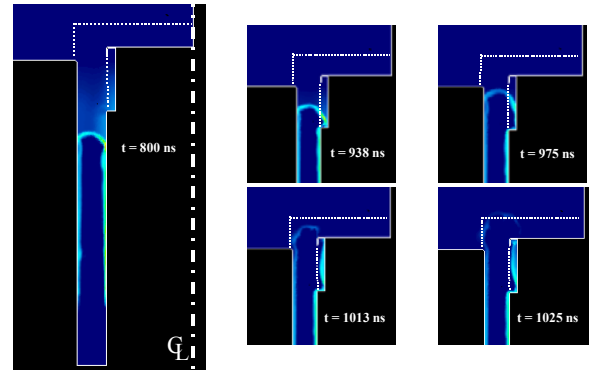

Figure 10. Typical plasma bridge density profiles near cathode for optimizing PRS load geometry.

IV. SUMMARY

Electrical circuit and MHD simulations were performed in support of the implementation of a MPOS on DQ. The circuit models suggest that an ACE 4 type POS-BRS configuration may achieve the goal of 290 kJ in the e-beam if downstream inductance is decreased by 50% and if the POS open impedance is increased by a factor of two. Existing ACE 4 data imply that the reduced inductance should be achievable. MHD models let us expect that with I_C*T_C = constant scaling, higher open impedance can be reached with simple changes in the downstream geometry of the POS. Such changes should benefit both hard x-ray BRS and soft x-ray PRS loads.

V. REFERENCES

[1] J. Thompson et al, "Decade Quad Monolithic POS Development on ACE 4," 12th IEEE Int. Pulsed Power Conf., Monterey, CA, 1999, pgs.210-313.
[2] J. Thompson et al, "Use of the Microsecond Inductive Energy Based ACE 4 Generator for 100 ns Z-pinch Loads," presented at APS DPP Annual Meeting, Oct. 2000.